

# Thermal tuning of a fixed Bragg grating for IR light fabricated in a $\text{LiNbO}_3:\text{Ti}$ channel waveguide

J. Hukriede, D. Kip, E. Krätzig

Fachbereich Physik, Universität Osnabrück, D-49069 Osnabrück, Germany  
 (Fax: +49-541/969-3510, E-mail: joerg.hukriede@uos.de)

Received: 1 April 1999/Published online: 24 June 1999

**Abstract.** We investigate a thermally tunable integrated narrow-bandwidth interference filter for light in the infrared wavelength region around  $\lambda = 1550$  nm fabricated in a channel waveguide in lithium niobate. The filter is based on a holographically recorded and thermally fixed refractive-index Bragg grating. The device is connected to optical single-mode fibers and works polarization-independent. We measure a peak reflectivity of 95% and a linewidth (FWHM) of 0.09 nm. By temperature-controlling the peak wavelength of the filter is tuned. For the linear thermal expansion coefficient of lithium niobate along the  $c$  axis the value  $\alpha_{33} = (4.5 \pm 0.5) \times 10^{-6} \text{ K}^{-1}$  is obtained. Permanent illumination of the filter with incoherent light allows us to adjust the peak reflectivity.

**PACS:** 42.40.Eq; 42.82.-m; 42.82.Et

Thermally fixed refractive-index gratings in iron-doped lithium niobate channel waveguides are of considerable interest in integrated optics. Reflection gratings for infrared light around  $\lambda = 1550$  nm can be recorded in photorefractive waveguides with visible green light utilizing holography [1]. Thereby the technique of thermal fixing (see, for example, [2]) allows us to enlarge the lifetime of the holograms. Protons are redistributed during writing at  $T \approx 450$  K and compensate for the generated space-charge field. After cooling down, homogeneous illumination with incoherent light generates modulated photocurrents arising from a modulated concentration of  $\text{Fe}^{2+}$  and  $\text{Fe}^{3+}$  ions. A space-charge field builds up again and forms a fixed refractive-index pattern via the linear electrooptic effect. Fixed Bragg gratings can help to build up dense WDM (wavelength division multiplexing) systems for optical communications or serve as highly spectral-selective laser mirrors for integrated waveguide DBR (distributed Bragg reflection) lasers in lithium niobate [3]. In this contribution we report on the thermal tuning of an integrated narrow-bandwidth wavelength filter recorded in a titanium-indiffused channel waveguide in iron-doped lithium niobate.

## 1 Experiment

The channel waveguide was fabricated in the following way: An undoped  $y$ -cut lithium niobate wafer of congruently melting composition was cut into pieces of  $7 \times 16$  mm, the  $c$  axis of the crystals pointing along the larger side. A 10-nm-thin layer of iron was deposited by thermal evaporation on the top face of one sample. We diffused the layer into the substrate for 48 h at a temperature of 1273 K in air to increase the concentration of photorefractive centers that participate in the charge transport during the holographic recording process. The channel was created by electron beam deposition of 100 nm titanium on the iron-doped side of the sample. With the help of photolithography followed by a chemical wet-etching process we defined a  $6\text{-}\mu\text{m}$ -wide titanium strip along the  $c$  axis of the crystal. It was indiffused for 18 h at 1273 K in air resulting in a single-mode waveguide for  $\lambda = 1550$  nm whose effective refractive indices for  $\text{TE}_0$  and  $\text{TM}_0$  nearly coincide. During the two diffusion processes nearly all of the iron in the sample had turned into the oxidized valence state  $\text{Fe}^{3+}$ . We increased the  $\text{Fe}^{2+}$  concentration by a final annealing treatment for 2 h at 1273 K in an argon atmosphere. Here the gas bubbled through water to increase the proton concentration  $c_{\text{H}^+}$ . Absorption measurements with a Fourier spectrometer [4] along the  $y$  axis of the sample yielded  $c_{\text{H}^+} = 5.3 \times 10^{24} \text{ m}^{-3}$ . Due to the measurement geometry this is an average value for the whole crystal including channel waveguide and substrate material. With the help of diffusion theory [5] we calculated an almost constant iron concentration of  $c_{\text{Fe}} = 2.3 \times 10^{25} \text{ m}^{-3}$  in the waveguiding channel.

The holographic grating in the sample was recorded and thermally fixed with nearly the same holographic two-beam setup as presented in [1]. We utilized an active stabilization system to keep the phase of the two beams constant in time. Further improvements in the thermal stability of the recording setup (base of the heatable crystal holder is now water-cooled) allowed us to reduce the writing time for the hologram to 37 min. The recording angle was  $2\theta = 93.83^\circ$ , the laser wavelength 514.5 nm, and the light intensity  $1500 \text{ W m}^{-2}$ . During recording the sample was kept at a temperature of 453 K. After cooling down to room tempera-

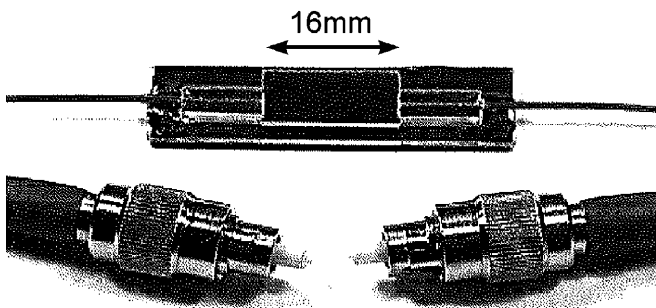


**Fig. 1.** Photograph of the investigated 16-mm-long waveguide interference filter. The device is connected to optical fibers on both sides and mounted on an object holder to increase its stability.

ture within 5 min, the hologram was developed with the white light of a 150-W halogen lamp for 30 min.

In a last step the waveguide was connected to optical single-mode fibers via its polished endfaces. The lithium niobate sample and the two bare fiber ends were fixed together with an UV adhesive. The two fiber connectors have a defined slant angle of  $8^\circ$  to minimize back reflections. The waveguide, however, was polished rectangular. The total transmission of the device from connector to connector in the off-Bragg case is about 30%, resulting in an insertion loss of 5 dB. This high loss results mainly from an insufficient quality of the endfaces and a slight misalignment of the fibers. On the other hand, lithium niobate is nearly transparent for the used infrared light, absorption in the channel will be almost negligible. A photograph of the device is shown in Fig. 1.

## 2 Results

Figure 2 shows a typical normalized transmission spectrum  $T(\lambda)$  of the filter for unpolarized light between  $\lambda = 1555.36$  and  $1559.36$  nm. We utilize a DFB laser with an optical isolator that is tunable in steps of  $0.01$  nm. The linewidth of the laser is smaller than  $2 \times 10^{-4}$  nm. At a center wavelength of  $\lambda_p = 1557.84$  nm the Bragg condition for readout in reflection geometry is satisfied. The reflectivity of the filter reaches  $\eta \equiv 1 - T(\lambda_p) = 95\%$  and the linewidth is  $0.09$  nm (FWHM). The large distortion of the signal (see inset) results

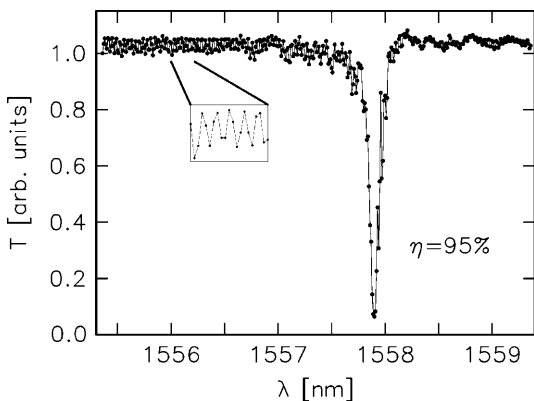


**Fig. 2.** Normalized transmission  $T$  of the interference filter versus wavelength  $\lambda$ . The distortion of the signal results from Fabry-Pérot interferences

from Fabry-Pérot interferences because the rectangular polished waveguide forms a resonator for the traveling light.

In Fig. 3 we present the corresponding reflection spectrum  $R(\lambda)$ . It was measured with the help of a 3-dB coupler which was inserted between the laser and the integrated wavelength filter. The center wavelength and the linewidth are the same as for the transmission curve. We also observe an additional constant background resulting from Fresnel reflections at the transitions between optical fibers and the lithium niobate waveguide.

Figure 4 represents the extracted peak wavelengths  $\lambda_p$  of the filter versus the temperature  $T$  of the sample environment. The data follow a straight line. A linear interpolation of the form

$$\lambda_p(T) = \lambda_p(T_0)(1 + \alpha_{33}(T - T_0)) \quad (1)$$

yields the thermal tuning coefficient  $\alpha_{33} = (4.5 \pm 0.5) \times 10^{-6} \text{ K}^{-1}$  of the device. The peak wavelength  $\lambda_p$  depends on the effective refractive index  $n_{\text{eff}}$  and the grating period  $\Lambda$  via the relation

$$\lambda_p = 2n_{\text{eff}}\Lambda. \quad (2)$$

If we neglect the temperature dependence of  $n_{\text{eff}}$  for the infrared light in the investigated temperature range [6] the shift in the peak wavelength results only from the thermal expansion of the sample and  $\alpha_{33}$  will be the thermal expansion coefficient of lithium niobate along the  $c$  axis. Our

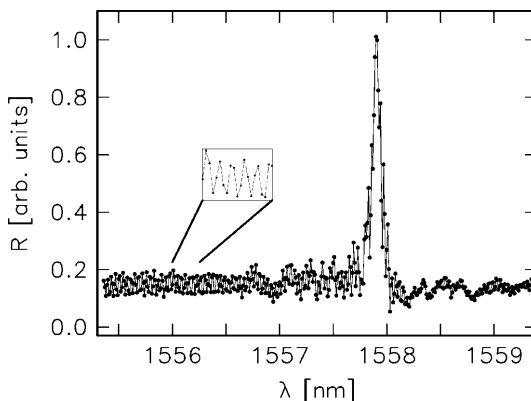


**Fig. 3.** Corresponding normalized reflected signal  $R$  of the interference filter versus wavelength  $\lambda$ . The constant background results from Fresnel reflections at the transitions between fiber and waveguide

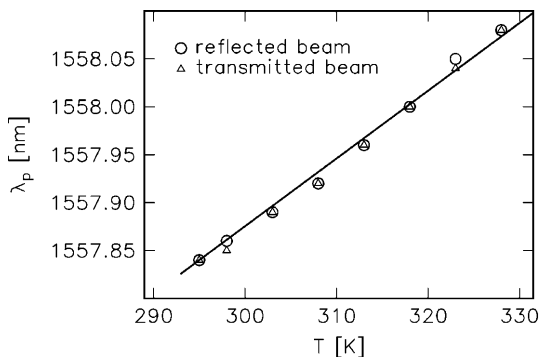


**Fig. 4.** Peak wavelength  $\lambda_p$  of the device versus temperature  $T$

measured value for  $\alpha_{33}$  is in good agreement with the value  $\alpha_{33} = 4.8 \times 10^{-6} \text{ K}^{-1}$  derived from [7].

A fast dark-relaxation of the developed refractive index grating is observed. Various transmission curves  $T(\lambda)$  were taken over time and from each peak reflectivity  $\eta$  we calculated the corresponding refractive index modulation  $\Delta n$  by the formula [8]

$$\Delta n = \frac{\lambda_p \operatorname{arctanh} \sqrt{\eta}}{\pi d}. \quad (3)$$

Here  $d = 16 \text{ mm}$  is the filter length. The result is shown in Fig. 5. The degradation of  $\Delta n$  does not follow a monoexponential law. The solid line is a fit to a biexponential function. However, we observe that a new developing process with the white light of the halogen lamp builds up the grating to its initial efficiency again. This means that the developed space-charge field is only compensated via the considerably high dark conductivity in the channel [9]. The long-term stability of the filter will be governed by a direct erasure of the protonic grating itself resulting from a remaining mobility of protons even at room temperature. This effect has not been investigated so far. The dark compensation mechanism of our grating is more than 20 times faster than that observed in [1]. The large iron concentration in the channel (about 50% more than in [1]) may be responsible for this effect. A future plan is to investigate in detail the influence of the iron concentration and the reduction state  $c_{\text{Fe}^{2+}}/c_{\text{Fe}^{3+}}$  on the dark conductivity.

For permanent operation it is necessary to keep the device illuminated homogeneously with the light of, for example, a blue LED [10]. To estimate roughly the light intensity needed to keep the reflectivity of the fixed grating at a desired value  $\eta$ , we let the incoherent white light of the halogen lamp travel through a bandpass filter for blue light (center wavelength 494 nm, linewidth 9 nm) before it impinged on the sample. We then measured the decay of the filter efficiency under homogeneous illumination for different light intensities  $I_0$ . Before each measurement the device was completely recovered to  $\eta = 95\%$ . As a representative, the curve for  $I_0 = 16 \text{ W m}^{-2}$  is also presented in

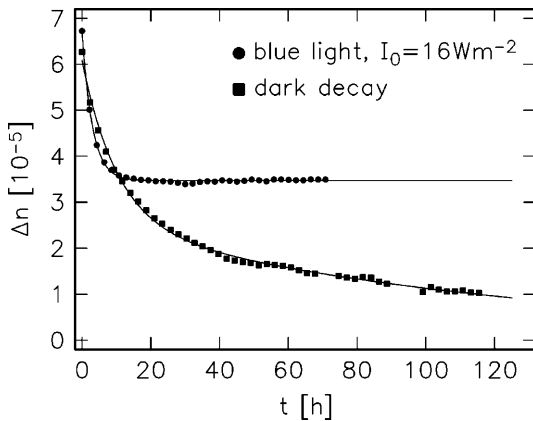


**Fig. 5.** Refractive index modulation  $\Delta n$  of the thermally fixed grating versus time  $t$ . *squares*: waveguide left in the dark; *circles*: waveguide illuminated with incoherent blue light. The dark decay was fitted by a biexponential function, the decay under illumination by a monoexponential function (*solid lines*)

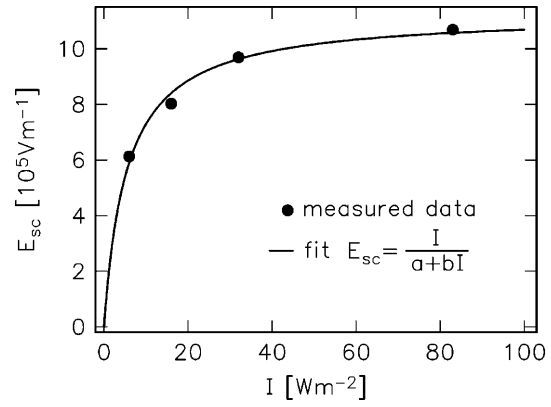


**Fig. 6.** Remaining space-charge field  $E_{sc}$  versus intensity  $I_0$  of the incoherent blue light used for permanent developing of the fixed grating

Fig. 5. After a certain time the signal no longer declined and a saturation refractive index modulation  $\Delta n_s$  was reached. From the measured values  $\Delta n_s(I_0)$  we calculated the corresponding electric space-charge field  $E_{sc}$  in the waveguide via the relation

$$E_{sc} = \frac{2\Delta n_s}{n_{\text{eff}}^3 r}, \quad (4)$$

where  $r$  denotes the linear electrooptic coefficient. The results are shown in Fig. 6. The solid line is a fit function following the relation  $E_{sc} = I_0/(a + bI_0)$ . This indicates that by simply varying the light intensity  $I_0$ , the remaining efficiency of the fixed grating can be regulated to a desired level. For the highest blue light intensity of  $I_0 = 83 \text{ W m}^{-2}$  a filter reflectivity of  $\eta > 80\%$  was preserved.

### 3 Conclusion

We report on the investigation of an integrated narrow-bandwidth interference filter for infrared light around 1558 nm. The device works polarization-independent and is attached to common optical single-mode fibers. It is easily tuned to a desired peak wavelength by precise temperature controlling. By permanent illumination with a blue-light LED the peak efficiency of the filter can be adjusted.

*Acknowledgements.* Financial support of the Deutsche Forschungsgemeinschaft (grant SFB 225, D9) is gratefully acknowledged.

### References

1. J. Hukriede, I. Nee, D. Kip, E. Krätzig: *Opt. Lett.* **23**, 1405 (1998)
2. K. Buse, S. Breer, K. Peithmann, S. Kapphann, M. Gao, E. Krätzig: *Phys. Rev. B* **56**, 1225 (1997)
3. C. Becker, A. Greiner, T. Oesselke, A. Pape, W. Sohler, H. Suche: *Opt. Lett.* **15**, 1194 (1998)
4. S. Kapphann, A. Breitkopf: *Phys. Status Solidi A* **133**, 159 (1992)
5. D. Kip, B. Gather, H. Bendig, E. Krätzig: *Phys. Status Solidi A* **139**, 241 (1993)
6. G.D. Boyd, W.L. Bond, H.L. Carter: *J. Appl. Phys.* **38**, 1941 (1967)
7. P.K. Gallagher, H.M. O'Bryan, E.M. Gyorgy, J.T. Krause: *Ferroelectrics* **75**, 71 (1987)
8. H. Kogelnik: *Bell Syst. Technol. J.* **48**, 2909 (1969)
9. D. Kip, J. Hukriede, E. Krätzig: *Phys. Status Solidi A* **168**, R3 (1998)
10. S. Breer, H. Vogt, I. Nee, K. Buse: *Electron. Lett.* **34**, 2419 (1998)